Past and Future Forcing of Beaufort Sea Coastal Change

Gavin K. Manson* and Steven M. Solomon

Geological Survey of Canada - Atlantic
1 Challenger Drive, Dartmouth NS B2Y 4A2

[Original manuscript received 9 December 2005; in revised form 22 January 2007]

ABSTRACT *Changes to the Beaufort Sea shoreline occur due to the impact of storms and rising relative sea level. During the open-water season (June to October), storm winds predominantly from the north-west generate waves and storm surges which are effective in eroding thawing ice-rich cliffs and causing overwash of gravel beaches. Climate change is expected to be enhanced in Arctic regions relative to the global mean and include accelerated sea-level rise, more frequent extreme storm winds, more frequent and extreme storm surge flooding, decreased sea-ice extent, more frequent and higher waves, and increased temperatures. We investigate historical records of wind speeds and directions, water levels, sea-ice extent and temperature to identify variability in past forcing and use the Canadian Global Coupled Model ensembles 1 and 2 (CGCM1 and CGCM2) climate modelling results to develop a scenario forcing future change of Beaufort Sea shorelines. This scenario and future return periods of peak storm wind speeds and water levels likely indicate increased forcing of coastal change during the next century resulting in increased rates of cliff erosion and beach migration, and more extreme flooding.*

RÉSUMÉ *[Traduit par la rédaction] Des changements dans la ligne de rivage de la mer de Beaufort se produisent sous l'effet des tempêtes et de la hausse relative du niveau de la mer. Durant la saison d'eau libre (de juin à octobre), les vents des tempêtes, principalement du nord-ouest, produisent des vagues et des marées de tempêtes qui parviennent à éroder les falaises riches en glace fondante et à produire un ennoiement des plages de gravier. On s'attend à ce que le changement climatique soit accentué dans les régions arctiques par rapport à la moyenne globale et qu'il entraîne une hausse accélérée du niveau de la mer, des vents de tempêtes extrêmes plus fréquents, des inondations causées par des marées de tempêtes plus fréquentes et plus extrêmes, une plus faible étendue de la glace de mer, des vagues plus fréquentes et plus hautes et des températures plus élevées. Nous étudions les relevés historiques de vitesse et de direction du vent, de niveaux d'eau, d'étendue de la glace de mer et de température pour déterminer la variabilité dans le forçage passé et nous utilisons les résultats de modélisation du climat des modèles couplés climatiques globaux 1 et 2 (MCCG1 et MCCG2) pour élaborer un scénario forçant le changement futur des lignes de rivages de la mer de Beaufort. Ce scénario et les périodes de retour futures des vitesses de vent de tempête et des niveaux d'eau de pointe indiquent selon toute probabilité un forçage accru du changement côtier durant le prochain siècle produisant de plus forts taux d'érosion des falaises et de migration des plages ainsi que des inondations plus extrêmes.*

1 Introduction

Long-term retreat of shorelines bordering the Beaufort Sea (Fig. 1) is considered to be driven by relative sea-level (RSL) rise (Héquette et al., 1995; Shaw et al., 1998; Solomon et al., 2000) caused by both isostatic subsidence and eustatic rise (Hill et al., 1993; Peltier, 1994; Manson et al., 2005). In the short-term (i.e., sub-decadal), rates of shoreline retreat are influenced by variability in external forcing and characteristics of the coastal morphosedimentary system (e.g., sediment availability, geotechnical properties, morphologic arrangement) (Héquette et al., 2001; Ruz et al., 1992; Hill et al., 1994).

During the October to June ice season, wave and surge development may be suppressed (Murty and Polavarapu, 1979), cliffs consisting of ice-bonded sediments are frozen, and shorelines are protected by shorefast and groundfast ice (Forbes and Taylor, 1994). In contrast, during the June to October open-water season, storm waves and surges may cause damage to coastal infrastructure (DPW, 1971; Berry et al., 1975; Lewis, 1987; Harper et al., 1988; Eid and Cardone, 1992). Waves superimposed on high water levels act upon thawed cliffs causing notch formation or reactivation of retrogressive thaw failures (Hill and Solomon, 1999; Dallimore et al., 1996). At the same time, depending partly upon the amount of beach-forming sediments delivered from eroding cliffs, barrier beaches and spits may grow or shrink in length and height (Hill et al., 1994; Forbes and Syvitski, 1994; Forbes et al., 1995).

*Corresponding author's e-mail: gmanson@nrcan.gc.ca

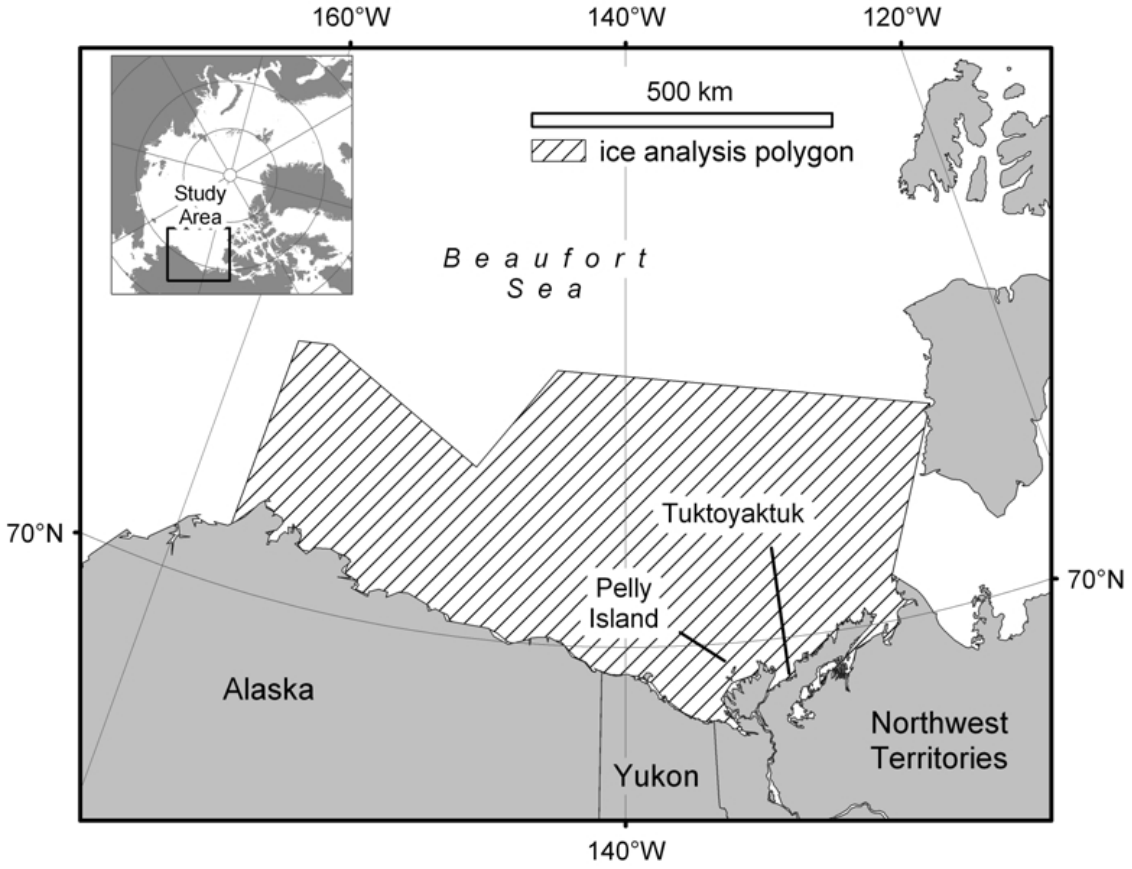

Fig. 1 Location map showing the study area. The hatched area shows the polygon used for ice analysis.

Relative to the global mean, climate change in Arctic regions is predicted to be enhanced (Räisänen, 2001). Though there is considerable uncertainty in regional sea-level change predictions, sea-level rise due to thermal expansion and increased meltwater contribution to ocean volume may be higher in the Arctic basin than the global average (Church et al., 2001). A rising trend in surface air temperatures that is strongly suggestive of anthropogenic forcing (Johannessen et al., 2002) began during the 1980s and is ongoing with implications for sea-ice extent. Johannessen et al. (2002) predict, from global coupled atmosphere-ice-ocean simulations using the European Centre Hamburg model version 4 (ECHAM4) of the Max Planck Institute for Meteorology (Roeckner et al., 1999) and the UK Meteorological Office HadCM3 model (Gordon et al., 2000), that summer sea-ice extent will decrease by 80% into 2100 when the Arctic Ocean will be essentially ice free in summer and multi-year ice will cease to exist. Northern hemisphere cyclone tracks are not expected to change though the frequency of intense cyclones may increase slightly in northern regions of cyclogenesis including the Sea of Okhost, Laptev Sea, East Siberian Sea and Beaufort Sea (Lambert, 2004; Lambert, 1995; McCabe et al., 2001). The combination of winds similar to present day with greatly increased amounts of open water and a longer open water season implies increased wave energy. When considered with increased temperatures and accelerated sea-level rise, increased forcing and accelerated change of Beaufort Sea and other Arctic shorelines are likely.

We present and investigate measured and modelled time series of wind speeds and directions, water levels, sea-ice extent and air temperature from the Beaufort Sea and Mackenzie Delta with a view towards understanding the characteristics of extreme, open-water season storms that have contributed to past coastal retreat and flooding. A potential future forcing scenario is developed from analyses of the respective time series and previous research results. Following on previous studies (e.g., Huntington et al., 2005), a five-tier likelihood of occurrence (very unlikely, unlikely, possible, likely and very likely) is assigned to each element in the scenario. Future wind and water-level event return periods are forecast by extrapolating current return periods based on the future climate scenario. The scenario is not necessarily a prediction of what will happen, but more a consideration of the types of impacts that could happen and their possible severity. It is intended to address an information gap identified by northern coastal communities and industries as they consider climate change impacts and develop adaptation strategies.

2 Data compilation and methods

To understand past variability in forcing, records of observed water levels (obtained from the Marine Environmental Data

Service), predicted tides (obtained from Fisheries and Oceans Canada, Central Arctic Region Data Acquisition Section), storm wave heights (Eid and Cardone, 1992), sea-ice extent (obtained from the Canadian Ice Service), wind speeds and directions, surface air pressures and surface air temperatures (obtained from the Meteorological Service of Canada) were collated in a database. Meteorological Station Inspection Reports were also obtained from the Meteorological Service of Canada. To contribute to a scenario of future forcing of coastal erosion, outputs from the Canadian Global Coupled Model ensembles 1 and 2 (CGCM1 and CGCM2; obtained from the Canadian Centre for Climate Modelling and Analysis; McFarlane et al., 1992; Flato et al., 2000; Flato and Boer, 2001) were similarly collated. Variables include predicted decadal sea-level rise, daily mean 10 m U and V wind speeds, monthly mean sea-ice concentrations and daily mean 2 m screen temperatures for the IS92a Greenhouse Gas plus Aerosol (GHG+A) scenario. In this scenario, CO_2 increases at the observed rate until 1996 and by 1% per annum thereafter (IPCC WG1, 2001) and the direct effect of sulphate aerosols is included by increasing albedo (Reader and Boer, 1998). Use of a single model and scenario does not demonstrate the large variability in model results (e.g., Wang and Swail, 2006; Räisänen, 2001) yet, in a five-model comparison including CGCM2 and specifically relating to the Arctic, all models tested were qualitatively consistent (Kattsov et al., 2005). More scatter was found between scenarios than between models; the IS92a scenario produced relatively small temperature changes (IPCC WG1, 2001). Since steric sea-level rise, decreasing sea ice and changing storminess can be considered derivative impacts of increasing temperature, the future forcing scenario could be considered conservative.

a *Water Levels and Surges*

Measurements in the hourly water level record from the Tuktoyaktuk tide gauge between 1961 and 1997 are often missing (approximately 45% of measurements) or spurious; obviously erroneous measurements consisting of spikes and other anomalies were removed. The record is most complete and accurate during the open-water season upon which our analyses focus. Open-water season water-level events defined by at least one hour of water level in excess of 1.25 m above chart datum were extracted along with corresponding wind and sea-ice statistics. Water levels were converted to surge heights using predicted astronomical tides and a list of open-water season surges greater than 0.7 m for at least six hours was compiled. Surge heights were used in the correlation and multiple regression analyses, whereas water level above chart datum was used in the flooding analyses.

Three CGCM1 ensembles of decadal steric sea-level change for 30 marine grid cells in the Beaufort Sea (71.81°N to 75.57°N and 127.46°W to 144.38°W) were averaged to obtain mean estimates of decadal sea-level rise between 1901 and 2091. Model results were referenced to chart datum using the average of annual mean sea levels for years with mostly complete data, and referenced to 1981 near the mid-point of the time series.

b *Wave Energy*

In a previous study of extreme wave events in the Beaufort Sea (Eid and Cardone, 1992), hindcast wave heights were determined for 30 storms between 1957 and 1988. Maximum significant hindcast wave heights at a grid node north of Pelly Island (node 411) were obtained for each of these storms that coincided with a wind event in our list (Appendix). For considerations of future wave climate, because no reliable wave predictions are available for the study area, we use open-water extent and wind speed as proxy data.

c *Wind Speed and Direction*

Three stations at Tuktoyaktuk were merged (with preference given to the Distant Early Warning (DEW) Line and automatic stations) to give a record from 1958 to 2000. Data prior to 1997 are irregular, either taken hourly, every four or six hours or with no data archived between 23:00 and 06:00 MST.

Hourly winds with little missing data are available from an automated station on Pelly Island beginning in 1994. Pelly Island winds have considerably higher speeds and variability than at Tuktoyaktuk and thus are likely to be more representative of marine winds. To extend the Pelly Island record back in time, the merged Tuktoyaktuk wind speed record was first normalized using its 1958–2000 mean and standard deviation and then reconstructed to the 1994–2000 mean and standard deviation of the Pelly Island record, thus creating a Tuktoyaktuk wind history with the mean and variance of Pelly Island. Wind directions were not altered. The resulting synthetic Pelly Island wind record utilizes the normalized and reconstructed Tuktoyaktuk DEW Line station (#2203910, 1958 to June 1993), the normalized and reconstructed Tuktoyaktuk Airport station (#2203912, July to October 1993) and the Pelly Island automatic station (#2203095, 1994 to 2000). In a six-year period of overlap, synthetic Pelly Island data fall within a mean of 1.6 km h^{-1} of measured Pelly Island data although individual hourly readings may differ by as much as 60 km h^{-1}, likely reflecting differing arrival times of storms at Pelly Island and Tuktoyaktuk.

The Station Inspection Reports show that between 1958 and 1993, the DEW Line station anemometer was actually located at Tuktoyaktuk airport at an elevation of 10.9 m above ground; it is not known to have been moved. In 1993, the airport station was located within a few hundred metres of the DEW Line anemometer at an elevation of 10 m above ground, but with a different type of anemometer. The Pelly Island station was never moved during the time interval of interest, but the anemometer type was changed. Changing anemometer types is assumed to have a negligible effect on record quality.

Wind events defined by at least six hours of speeds greater than 50 km h^{-1} were extracted from the synthetic Pelly Island wind record and a subset of open-water season events (June to October) and north-westerly open-water (NWOW) season events with a mean direction from the north-west (270° to 360°). The speed and direction criteria were selected to reflect the finding that winds greater than 50 km h^{-1} have a modal north-westerly direction, the wind direction associated with

storm surges and resulting coastal impacts. A six-hour duration was selected because most of the record consists of six-hourly readings and to limit aliasing event frequencies towards hourly data; nevertheless, event frequencies were found to be lower in a six-hourly decimated dataset compared to the undecimated hourly dataset, suggesting that more storms occurred prior to 1994 than are identified here, and particularly during the open-water season of 1993 when the airport station was not operating at night. No attempt was made to correct for aliasing due to measurement spacing.

If available, corresponding information including storm duration, mean storm wind speeds, directions and water levels, peak storm wind speeds and their directions, maximum storm water levels, maximum hindcast wave heights, minimum storm air pressure, and the amount of open water the week of the storm were also extracted.

Daily mean U and V wind speeds at an elevation of 10 m output from CGCM1 (ensemble 1) were obtained for a marine grid cell in the Beaufort Sea north of Pelly Island centred at 72.36ºN, 135.00ºW. To render modelled and measured winds comparable, the model wind speeds were first normalized to their 1961 to 1990 mean and then reconstructed using the 1961 to 1990 mean of the synthetic Pelly Island wind record. We analyse the model output with respect to deviations from its 1961 to 1990 mean.

d *Sea Ice Concentration*

Weekly digital ice charts between mid-June and mid-October from 1968 to 1998 were obtained from the Canadian Ice Service. In a Geographic Information System (GIS)-based analysis, a polygon was superimposed over an area of interest (Fig. 1) approximately covering the summer extent of the Beaufort Sea coastal polyna and, for each weekly chart, the areas of open water (considered to be ≤ 5/10 ice cover) and ice (considered to be >5/10 ice cover) were determined (on ice charts, 0/10 ice is completely open water and 10/10 ice is complete ice cover). Charts were not produced between November and May and ice cover is assumed to be total.

Three CGCM2 ensembles of monthly mean sea-ice concentrations were obtained for nine grid cells closely matching the area of the GIS-based analysis and averaged.

e *Air Temperature*

Surface air temperatures obtained for the three Tuktoyaktuk stations were combined into a record spanning 1958 to 2000 with missing data during the winter of 1993/94. The DEW Line station temperature screen was located about 1.6 km north-east of the automatic and airport stations and shows a 0.2°C mean difference (cooler at the airport station) in overlapping values (H. Melling, personal communication, 2006); no alterations were made to the air temperatures during the merging of records. Preference was given to the DEW Line and automatic stations rather than the irregularly operated airport station.

Screen temperatures at an elevation of 2 m for three CGCM2 ensembles of the same grid cell as the modelled wind data were also obtained and averaged. No adjustments were made to modelled surface air temperatures. Model results are considered with respect to deviations from their 1961 to 1990 mean.

f *Air Pressure*

Air pressures were also obtained from the three Tuktoyaktuk stations and combined in a record corresponding to the air temperature record. As with temperature, there may be differences between stations due to spatial separation of the barometers; over 1.6 km the mean difference is assumed to be negligible and no alterations were made to station pressure. Air pressure is used in the correlation and multiple regression analyses to attempt to explain some of the variability in storm surge heights.

g *Correlation and Regression*

To identify which storm characteristics contribute to large surges, we tested the correlation between peak storm wind speed, mean storm wind direction, sea-ice extent, minimum storm air pressure, and peak storm surge height for identified open-water season wind events. Significantly correlated variables were chosen for stepwise multiple regression to determine the influence of wind speed, wind direction, air pressure and sea-ice extent on peak storm surge heights.

h *Return Period Analysis*

Because of the relatively limited number of years of overlapping wind, water level and sea-ice records (1971 to 1997) and lengthy periods of missing data, we adopted the Peaks-Over-Threshold (POT) method (Heckert and Simiu, 1996; Pandey et al., 2001) as opposed to the Annual Maxima method (e.g., Eid and Cardone, 1992) to predict wind and water level return periods. In the POT method, all available events are utilized instead of a single event per given time interval.

The Method of L-Moments (e.g., Reiss and Thomas, 2001) was used to fit the three-parameter Generalised Pareto Distribution (GPD) to wind events with a peak speed ≥ 60 km h^{-1} and water level events ≥ 1.25 m above CD as given by (Pandey et al., 2001):

$$\mathrm{Prob}(Y < y) = 1 - \left[1 + \frac{c(y-h)}{a}\right]^{\frac{-1}{c}} = 1 - \frac{1}{rT} \qquad (1)$$

where c and a denote the shape and scale parameters determined during distribution fitting and h, the location parameter, is equal to the threshold, r is the annual mean crossing rate of the threshold (i.e., the mean number of times the threshold is exceeded per year) and T is the return period in years. Both the wind speed and water level peaks over threshold were well fit by the GPD. Equation (1) can be rearranged to solve for the value of y at each return period T following

$$y = \frac{a\left[\left(rT\right)^{c} - 1\right]}{c} + h. \qquad (2)$$

Return periods of water level and wind events were calculated for 2000, 2050 and 2100. For water-level return periods

in 2000, we analysed peak water levels over threshold in the event list. For 2050 and 2100 we assume constant subsidence and accelerated eustatic rise due only to steric contributions. CGCM2 model results indicate 0.40 m of steric sea-level rise in the Beaufort Sea between 1991 and 2091. Globally averaged CGCM2 steric sea-level rise given by Church et al. (2001) is 0.11 m for the period 1990 to 2040 and 0.33 m for the period 1990 to 2090, indicating that 67% of sea-level rise may occur during the latter part of this century. Future Beaufort Sea RSL rise is then the sum of the current RSL rise of 3.5 mm y^{-1} (see Section 3a) plus a steric increase of 0.13 m by 2050 and a further 0.27 m steric increase by 2100 (for a total 0.4 m steric rise). This gives an RSL rise of 0.31 m by 2050 and 0.76 m by 2100 which were added to the location parameter to reflect the amount of sea-level rise since 2000.

For wind-event return periods in 2000, we analysed peak wind speeds over threshold in the NWOW event list. For 2050 and 2100, with the rationale that forcing is a combination of wind and open-water extent, we investigated CGCM1 and CGCM2 wind speed and sea-ice parameters. Lambert (2004) predicts that, though overall northern hemisphere cyclone frequency is expected to decrease linearly by approximately 3% in a $2xCO_2$ scenario between 2000 and 2100, the frequency of intense cyclones (i.e., the top 5% of events) may increase linearly by approximately 17% between 2000 and 2100 in typical regions of cyclogenesis affecting the Beaufort Sea. CGCM2 peak sea-ice concentrations in the Beaufort Sea by 2100 are similar in magnitude to peak sea-ice concentrations predicted by CGCM2 for the present day Gulf of St. Lawrence (Manson et al., 2002), suggesting that an April to December open-water season will exist in the Beaufort Sea. For the return period analysis in 2050, we therefore recalculated the Pareto parameters for the peaks over threshold in the NWOW wind event list but included November and May north-westerly events and decreased the number of occurrences of all events by 1.5% and increased the frequency of occurrence of the upper 5% of storms by 8.5%. For 2100 we again recalculated the Pareto parameters for the NWOW event list, this time including December and April storms, decreasing the number of occurrences of all events by 3%, and increasing the frequency of occurrence of the upper 5% by 17%.

3 Results and discussion

a *Relative Sea-Level Rise*

Linear regression of the monthly mean water levels for months with more than 90% complete data indicates that an RSL rise of 3.5 ± 1.1 mm y^{-1} has occurred at Tuktoyaktuk since 1961 (Fig. 2) which is statistically significant at α = 0.05. This rate is higher than the most probable estimate for the last 3000 years of 2.5 mm y^{-1} though it is less than the maximum possible rate of 4.4 mm y^{-1} (Hill et al., 1993). For the last 1000 years, the current rate is higher than both the most probable rate of 1.1 mm y^{-1} and the maximum possible rate of 2.5 mm y^{-1} (Campeau et al., 2000). This may suggest that acceleration in the rate of the RSL rise has occurred relative to the last 1000 years that may be attributable to increased rates of subsidence, accelerated eustatic sea-level rise, or both.

Comparison of measured and modelled sea levels (Fig. 3) shows most decadal modelled results lie within one standard deviation of measured annual means and that the trend in RSL is similar. CGCM2 includes only steric expansion, that portion of RSL rise due to thermal expansion of the top 1175 m (Bryan, 1996), and includes neither eustatic rise due to meltwater contribution to ocean volume nor isostatic subsidence. A similar trend may indicate an overestimation of steric rise by CGCM2, but the modelled area includes the Beaufort Gyre while measurements are made at the coast, so the two may not be directly comparable. As explained in Section 2h, total RSL rise is likely to accelerate, possibly giving a rise of 0.31 m by 2050 and a rise of 0.76 m by 2100.

b *Water Levels and Surges*

A time-time plot of water levels is shown in Fig. 4a. On average, the highest water levels occur during the open-water season; periods of high water levels appear to have occurred during the open-water seasons of 1968 to 1975, 1980 to 1985 and after 1990. Due to missing data, little can be said of the intervening periods.

Seventy-seven open-water season water-level events were identified. Coincidence of water-level events with wind events was poor; only 37 of the identified events coincided with identified NWOW wind events identified here and only 20 water-level events coincided with storms in previous compilations (Berry et al., 1975; DPW, 1971; Lewis, 1987; Eid and Cardone, 1992; Hudak and Young, 2002). Agreement was better when considering surges. Of the 51 surges in the surge event list, 37 coincided with identified NWOW events. Low coincidence of wind and water-level events may result from the separate or combined influences of missing data in the water-level record and the threshold levels chosen in this and other studies. Additionally, previous compilations considered moderate to weak events which were not necessarily from the north-west. Better agreement of surge events and wind events also points to the importance of astronomical tide in controlling flood levels, even in a micro-tidal environment such as Tuktoyaktuk. Surges which may bring elevated water levels are rare under conditions other than strong north-westerly winds. Correlation of surge heights with other storm parameters is further investigated quantitatively in Section 3g.

c *Wave Energy*

Of the 30 wave events hindcast by Eid and Cardone (1992), 14 correspond with Pelly Island NWOW wind storms identified in this study (Appendix). The wave events identified by Eid and Cardone (1992) include waves during wind events from all directions and are therefore not necessarily the most extreme events.

No continuous wave data from which a climatology can be constructed and no model results for future wave heights are

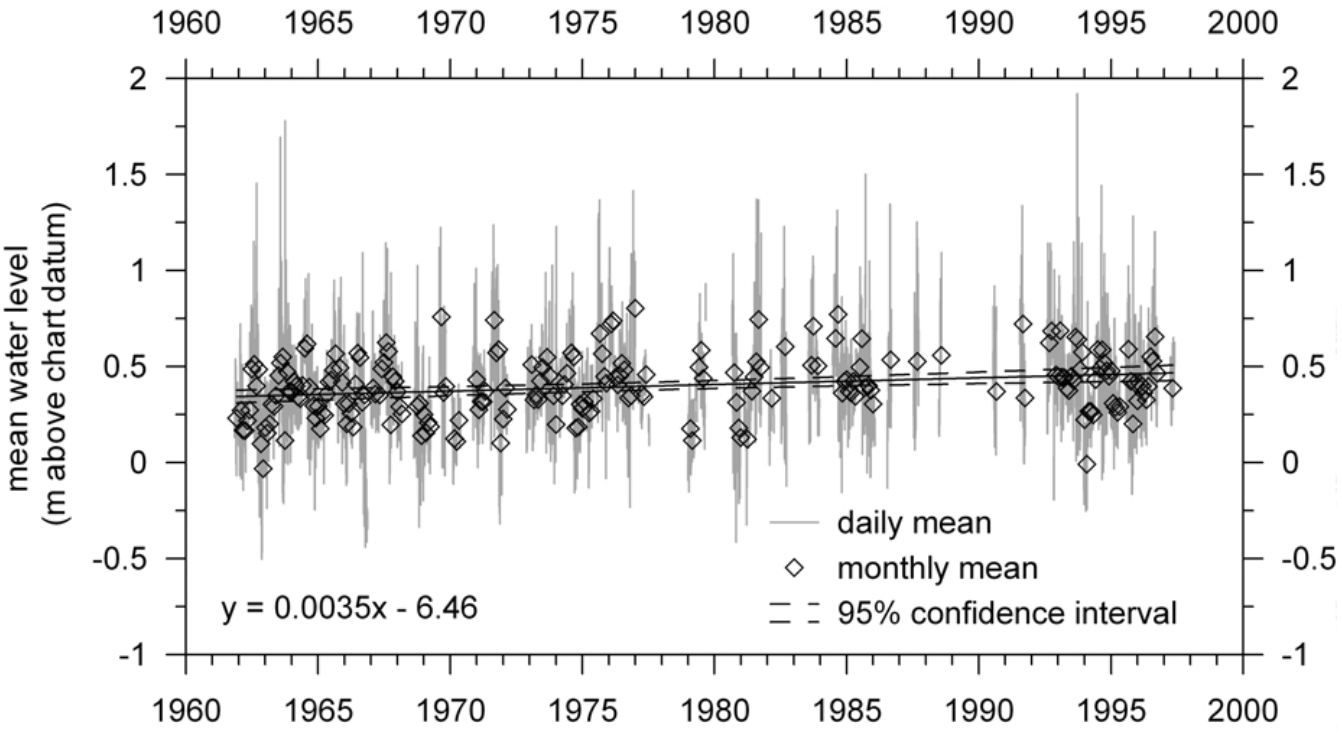

Fig. 2 Daily and monthly mean water levels measured at the Tuktoyaktuk tide gauge with gaps indicating missing data. Regression of the monthly means of years with nearly complete data indicates a statistically significant relative sea-level rise of 3.5±1.1 mm y^{-1}.

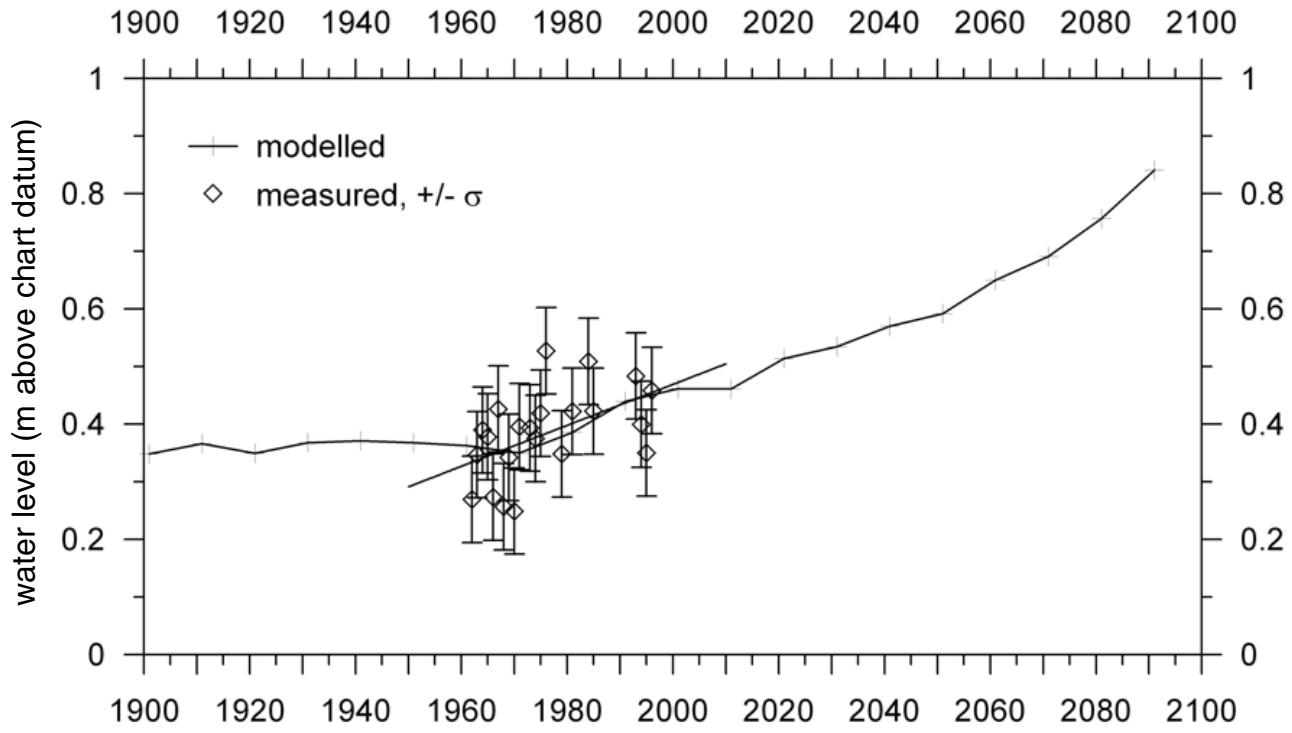

Fig. 3 Modelled and measured sea-level rise. Modelled includes only the steric portion while measurements include the components of RSL rise due to both land subsidence and the contribution of meltwater.

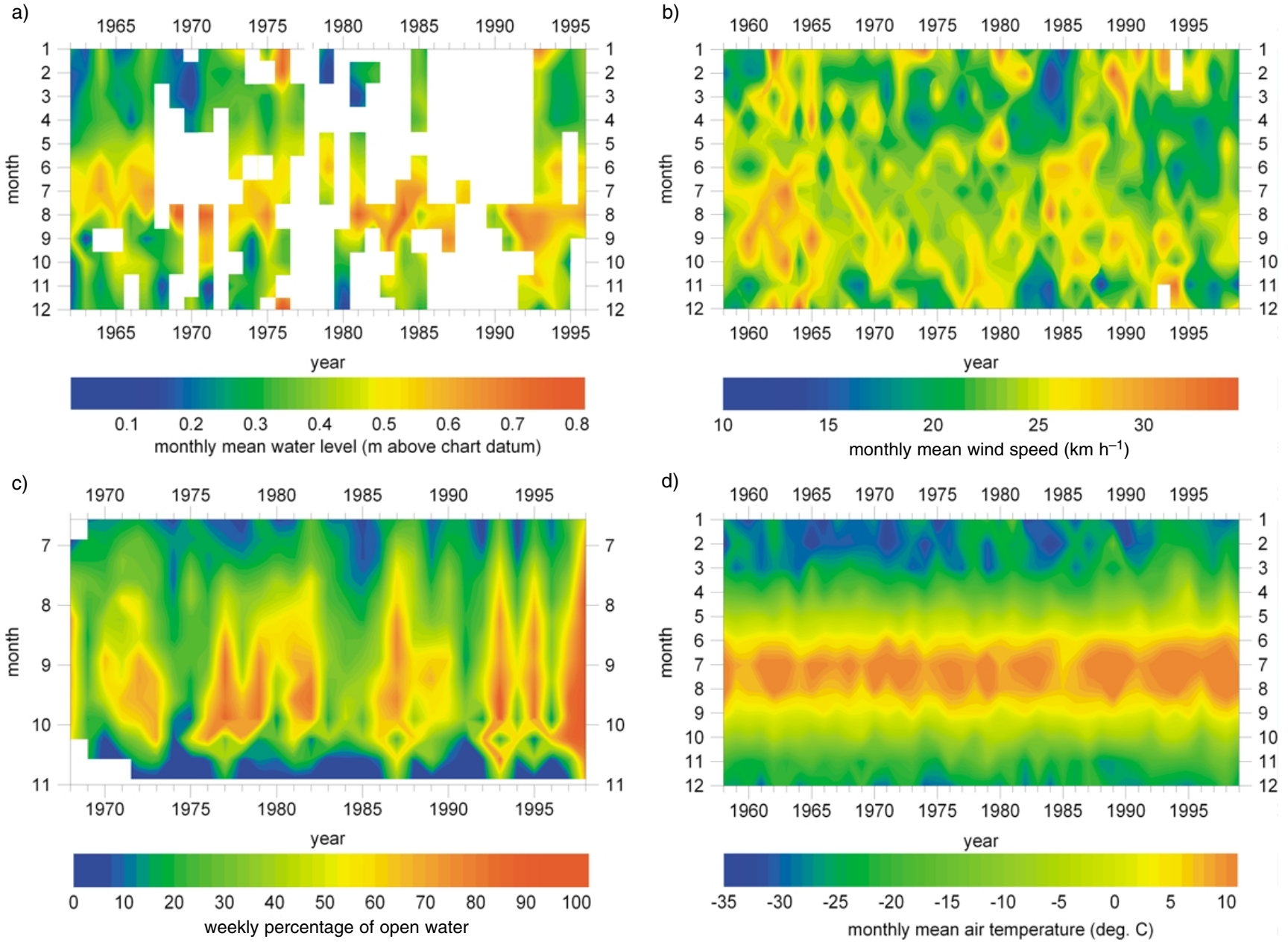

Fig. 4 Time-time plots of a) monthly mean water levels at Tuktoyaktuk, b) monthly mean wind speed in the synthetic Pelly Island record, c) weekly percentage of open water (defined here as ≤ 5/10 ice cover) during the Beaufort Sea open-water season, and d) monthly mean air temperatures at Tuktoyaktuk.

ATMOSPHERE-OCEAN 45 (2) 2007, 107–122 doi:10.3137/ao.450204
Canadian Meteorological and Oceanographic Society

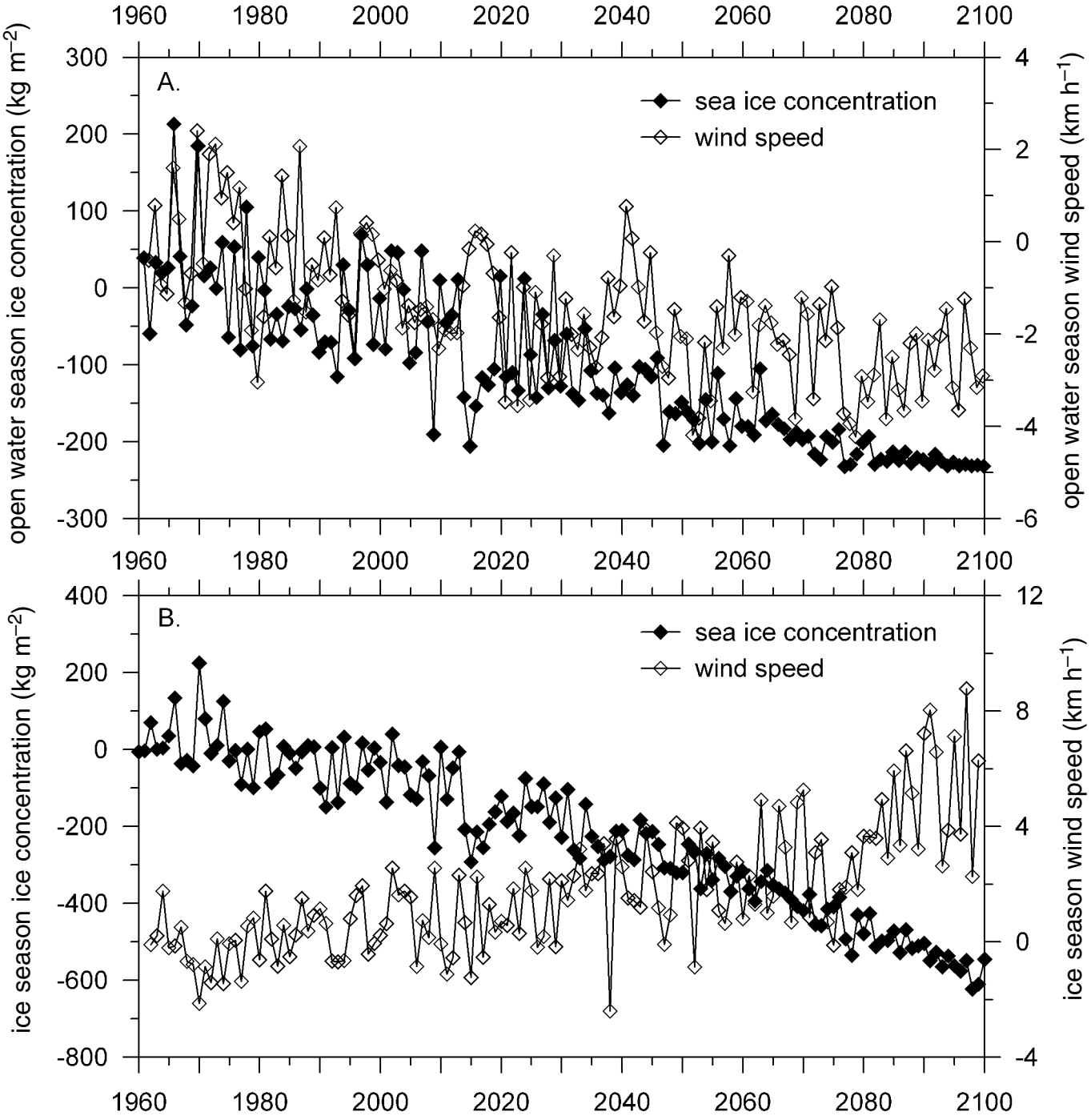

Fig. 5 Comparisons of modelled sea-ice concentration and wind speeds during the open-water and ice seasons (all expressed as deviations from their respective 1961 to 1990 means). Together these represent proxy evidence for increased wave energy at the beginning and end of the current open-water season and slightly reduced wave energy during the current open-water season.

available for the Beaufort Sea; modelled wind speeds and sea-ice extent are taken as proxy data for a qualitative estimate of the future wave climate. These are presented in Fig. 5 which suggests that wave energy will likely decrease between June and October as both seasonal mean wind speed and sea-ice concentrations decrease and that wave energy will likely increase (except when ice cover is extensive) between November and May when reduced mean sea-ice concentration is accompanied by accelerated mean wind speeds. It is noteworthy that the height of waves in the shallow Mackenzie Delta and Tuktoyaktuk region of the Beaufort may be depth-limited rather than fetch-limited such that decreasing sea ice may have little effect on wave height. However, a longer open-water season and increased wind speeds will cause increased wave energy at the coast, even though wave heights are similar, because waves have the potential to act for a

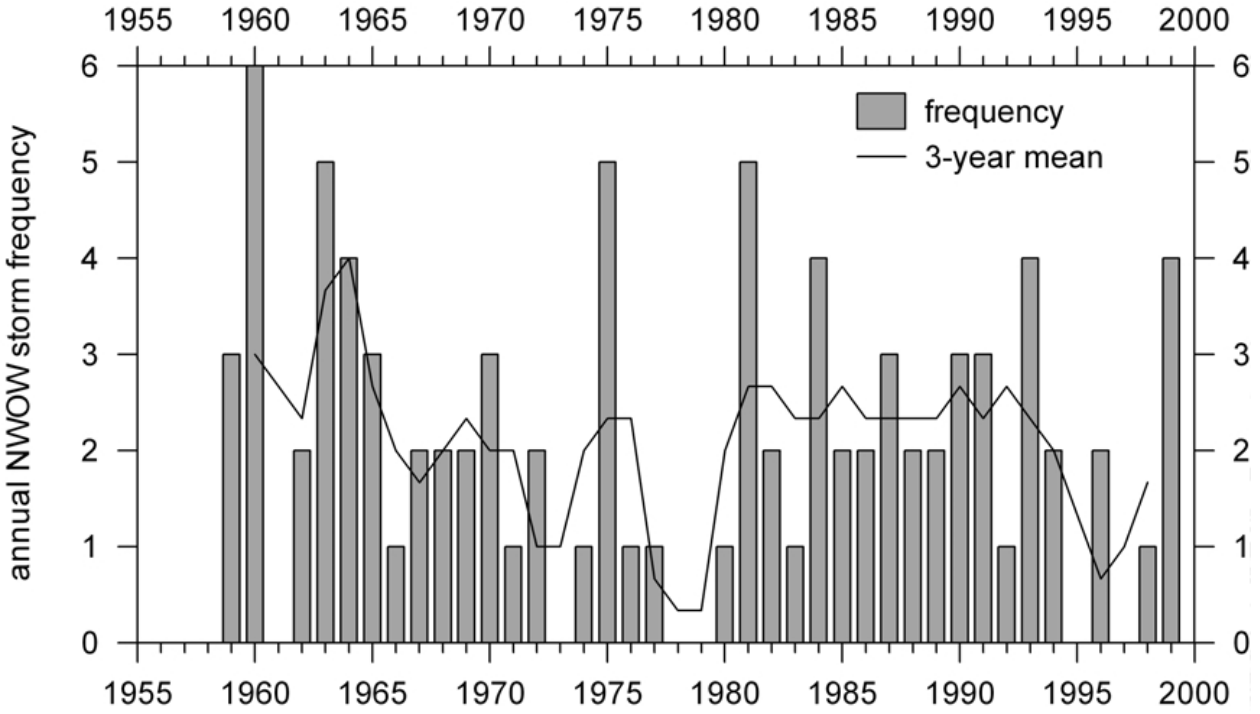

Fig. 6 Annual frequencies of NWOW wind storm events at Pelly Island and the three-year running mean.

longer portion of each year. Overall, wave energy impacting Beaufort Sea shorelines is likely to increase.

d *Wind Speed and Events*

A time-time plot of wind speeds (Fig. 4b) shows that high winds generally occur during the fall and winter and low winds occur during the summer, however, this pattern can vary and prominent calm periods can occur during the fall or winter and periods of increased winds can occur during the summer. A prominent period of elevated wind speeds occurred between 1960 and 1966 and a more subdued and variable period of elevated speeds occurred from 1986 to 1995. A period of increased wind speeds during the open-water season as well as several short periods of high winds during the ice season contributed to the 1960 to 1966 stormy period. The 1986 to 1995 stormy period is initially characterized by increased wind speeds throughout the open-water season but during the 1990s winds are generally calm during the early open-water season and stronger during the ice season. Periods of low wind speeds occurred during 1983 and 1984 and again after 1995. Calm periods are characterized by low wind speeds during both the open-water and ice seasons.

A total of 88 NWOW events exceeding 50 km hr^{-1} for at least six hours between 1959 and 1999 were identified (Appendix). Two additional events not in the compiled wind record (9 September 1944 and 10 September 2000) were also added to the list. The 1960 to 1966 stormy period is characterized by an increased annual frequency of events, but a similar increase during the more moderate 1986 to 1995 stormy period is less apparent (Fig. 6). Few events occurred during the 1983 to 1984 calm periods and a prominent period of few storm events occurred in the late 1970s. While this pattern is in some agreement with results from Lynch et al. (2004), it differs from the results of Hudak and Young (2002) mainly due to different storm selection criteria. We identify shorter-lived, more extreme events whereas Hudak and Young (2002) also identify longer-lived more moderate events. Of the NWOW storms identified here, 91% were also identified by Hudak and Young (2002) and the storms identified here may be considered an extreme subset of their Arctic type storms.

CGCM1 wind speeds were found to underpredict measured wind speeds at Pelly Island, potentially due to differing length scales of point measurements versus large-scale model results (http://www.cccma.bc.ec.gc.ca/data/cgcm1/cgcm1_ghga.shtml). CGCM1 modelled winds for the June to October and November to May seasons, expressed as departures from the 1961 to 1990 mean, are given in Fig. 5. By 2050 wind speeds are likely to have decreased slightly between June and October and increased between November and May. By 2100, the decrease in June to October winds is likely to have stabilized, though the increase in November to May wind speeds is likely to have accelerated.

As explained in Section 2h, by 2100, the most severe storms are likely to increase in frequency by possibly 17%, whereas the total occurrence of storms is likely to decrease by possibly 3%.

e *Sea Ice Concentration*

A time-time plot of weekly percentage of open water mapped between June and October shows that there is variability in

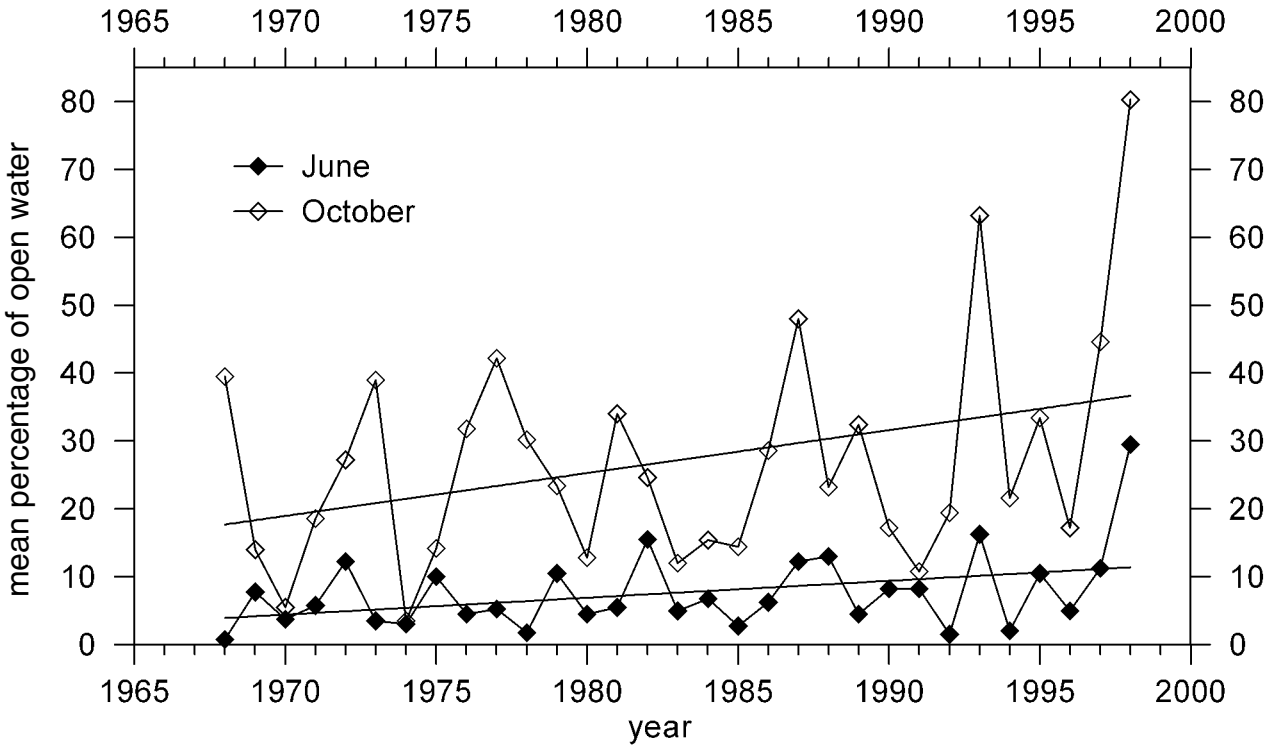

Fig. 7 Mapped monthly mean percentage of open water (≤ 5/10 ice cover) in June and October in the Beaufort Sea. The amount of open water during freeze-up and break-up is variable and appears to show a five-year cyclicity. A lengthening of the open-water season as indicated by more open water in June and October is apparent in recent years.

the timing of break-up, freeze-up, and in the maximum amount of open water that develops during a season (Fig. 4c). Typically, more open water develops when break-up is relatively early and freeze-up relatively late. Large amounts of open water occurred in the late 1970s to early 1980s, 1987 and also after the mid-1990s. Amounts of open water at break-up (mean June percentage of open water) and freeze-up (mean October percentage of open water) show considerable variability from year to year (Fig. 7), but it appears that freeze-up is more variable and presents a stronger apparent trend towards later freeze-up while the timing of break-up is less variable and presents a lesser apparent trend. Both are statistically insignificant.

Modelling and mapping results were not found to be comparable quantitatively due to different units (mapped results are in percentage by area whereas modelled results are in concentration by weight per unit volume). However, between 1969 and 1999, mapping and modelling results agree well in trend and magnitude of variability, though the two records differ in identifying heavy ice years and light ice years.

From CGCM2, decreases in sea-ice concentration are very likely during both the open-water and ice seasons (Fig. 5). By 2075, June to October concentrations are expected to possibly reach 0 kg m^{-3}, and by 2100, November to May concentrations are predicted to decrease and reach typical peak concentrations less than half those of 2000, possibly about 200 kg m^{-3}. This maximum is similar to present day ice-season maxima in the Gulf of St. Lawrence predicted by CGCM2 (Manson et al., 2002) which suggests that by 2100 the Beaufort Sea may possibly have a similar ice climate to the present day Gulf of St. Lawrence, that is, an open-water season from April to December with complete open water and a short ice season between January and March with discontinuous first-year ice cover.

f *Air Temperatures*

A time-time plot of monthly mean temperatures at Tuktoyaktuk (Fig. 4d) shows July to be the warmest month and January and February to be the coldest. Warm open-water seasons appear to have a periodicity of approximately five years and a trend may exist toward a lengthening of the warm season into late September and warming during the cold season.

Deviations of modelled monthly means from the modelled 1961 to 1990 mean of CGCM2 temperatures (Fig. 8) shows that air temperatures in the Tuktoyaktuk region are very likely to rise and that, by 2100, ice-season temperatures may possibly increase to approximately 14°C above the modelled 1961 to 1990 mean and open-water season temperatures to approximately 4°C above the modelled 1961 to 1990 mean. Freezing of sediments will still occur in winter as seasonal low temperatures will be below freezing but the duration of freezing will be shorter. In summer, mainly due to a lengthened thaw season rather than increased summer temperatures,

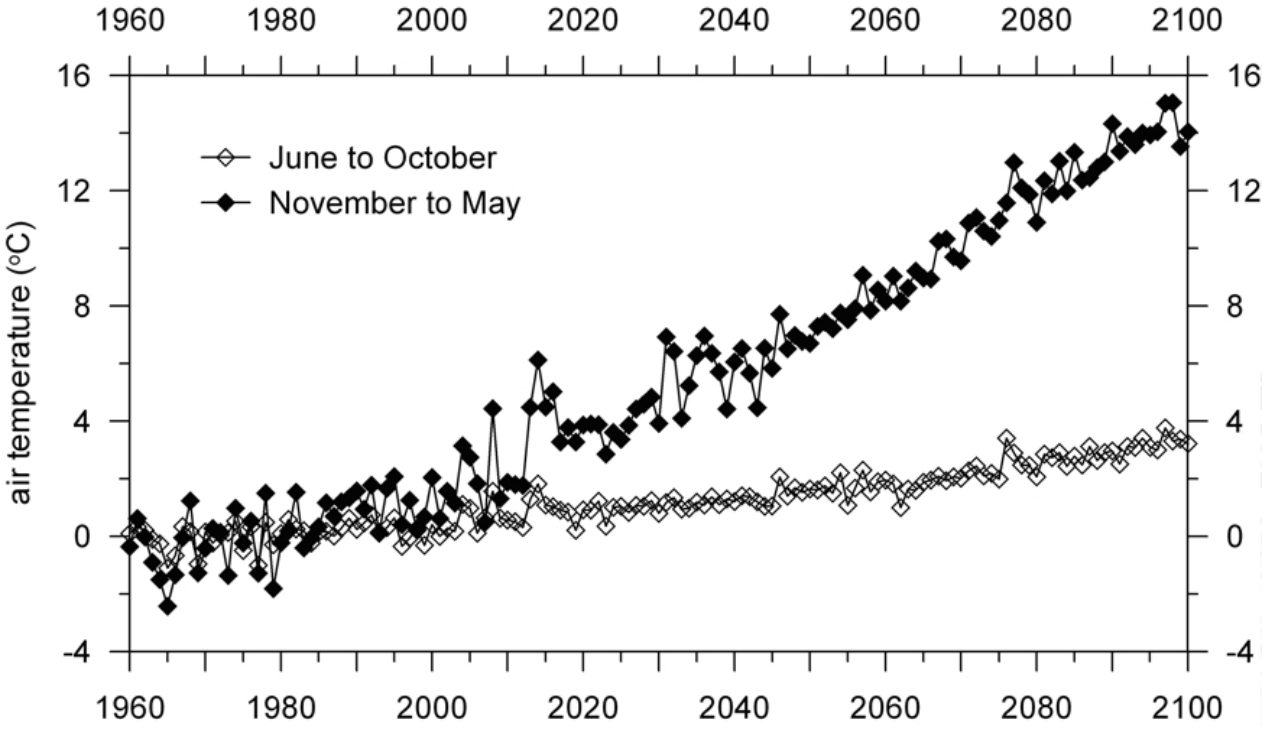

Fig. 8 Modelled surface air temperatures at Tuktoyaktuk. Temperatures are predicted to increase year-round with the largest increases occurring between November and May, suggesting a shortened freezing season and lengthened thaw season.

TABLE 1. Results of correlation test conducted on open water season storms. Significant correlations are shown in italics.

Variable $n = 54$ $\alpha = 0.05$	Peak Wind Speed (km h^{-1})	Mean Wind Direction	Open Water (%)	Minimum Air Pressure (kPa)	Peak Water Level (m above CD)
Peak Wind Speed (km h^{-1})	1.00	–	–	–	–
Mean Wind Direction (deg.)	0.13	1.00	–	–	–
% Open Water	*0.27*	0.05	1.00	–	–
Minimum Air Pressure (kPa)	*-0.42*	-0.20	-0.15	1.00	–
Peak Surge Height (m)	*0.52*	*0.69*	*0.30*	*-0.27*	1.00

TABLE 2. Results of stepwise multiple regression.

Variable	B	Model R^2	Partial Correlation	p-level
Mean Wind Direction (deg.)	0.693	0.480	0.750	0.000
Mean Wind Speed (km h^{-1})	0.437	0.668	0.551	0.000
% Open Water	0.159	0.691	0.269	0.056
Minimum Air Pressure (kPa)	0.057	0.694	0.091	0.525

thaw will likely penetrate deeper, thickening the active layer, and promoting active layer detachments and retrogressive thaw failure of ice-bonded slopes (Couture et al., 2002).

g *Relationships Between Winds, Water Levels, Air Pressure and Sea Ice*

Quantitative estimates of the contributions to variability in surge height at Tuktoyaktuk by Beaufort Sea open-water extent, Pelly Island wind speed and direction, and Tuktoyaktuk air pressure can be obtained through multiple regression. Variables for regression analysis were chosen based on the results of a correlation test (Table 1) which show that, for 54 open-water season wind events with water-level and ice data, peak surge height is significantly positively correlated ($\alpha = 0.05$) with peak wind speed, mean wind direction, percentage of open water and minimum air pressure.

In stepwise multiple regression, peak wind speed, mean direction and percentage of open water were found to significantly contribute ($\alpha = 0.10$) to the variance in surge height while the minimum air pressure during an event was not. With the first addition of mean wind direction, 48% of the variance in peak surge heights was explained. This increased to 67% with the second addition of mean wind speed, to 69% with the third addition of percentage of open water and

TABLE 3. Statistically modelled return periods of peak storm water levels (m above CD).

Return Period (years)	2000	2050	2100
2	1.77	2.08	2.53
5	2.00	2.31	2.76
10	2.16	2.47	2.92
25	2.36	2.67	3.12
50	2.51	2.82	3.27
100	2.65	2.96	3.41

TABLE 4. Statistically modelled return periods of peak storm wind speeds (km h^{-1}).

Return Period (years)	2000	2050	2100
2	73	74	79
5	82	83	87
10	88	89	92
25	95	96	99
50	101	101	103
100	105	106	108

insignificantly with the final addition of minimum air pressure (Table 2). The variability remaining unexplained could reflect the influence of water temperature, Mackenzie River discharge, the spatial distribution of open water and sea ice, and the speed, duration and particular track of the storm as it approaches the area.

The very minor contribution of open-water extent to elevated water levels may suggest that, during the open-water season, surges can develop even in the presence of extensive ice cover. Kowalik (1984) incorporated an ice edge into a storm surge model for the Beaufort Sea and found that there was little difference between predicted water levels with and without partial ice cover. Murty and Polavarapu (1979) consider that complete ice cover reduces coupling between the wind field and the water surface thus reducing wind stress and surge formation. Higher than predicted water levels have been measured under ice cover in recent years at the Tuktoyaktuk and Holman tide gauges; however, the degree to which ice cover affected amplitudes is not known. It is also possible that the 5/10 threshold selected to denote open water versus ice cover does not have a physical basis related to the processes of surge formation and propagation. The spatially averaged concentration may be less important than the configuration of ice with respect to the shoreline. The influences of sea ice on surge formation and propagation may not be adequately described by linear statistical models and remain poorly understood.

h *Future Forcing Scenario*

These results suggest a future forcing scenario which includes: likely RSL rise of possibly 0.31 m by 2050 and 0.76 m by 2100; very likely decreasing sea ice and an open-water season possibly lengthened to May to November by 2050 and April to December by 2100; unlikely change in storm tracks affecting the Beaufort; likely increased frequency of severe storms possibly occurring later in the year; likely overall increasing wave energy, likely with decreases in the summer months and increases in the spring and fall; and very likely increased air temperatures, likely with greater increase in the winter than the summer.

To further quantify this scenario, the results of the water-level return period analysis are incorporated (Table 3). With sea-level rise predicted in this scenario, flooding of low-lying areas on the Beaufort coast is very likely to become more common and more severe as the frequency of occurrence of a given water level increases. For example, the 25-year water-level event is currently expected to produce 2.36 m water levels (slightly less than the 1944 and 1970 storms). Without considering any change in storminess and ignoring the uncertain influence of sea ice on storm surge formation and propagation, by 2050, this water level is expected to occur every 5 to 10 years and by 2100 is expected to occur annually.

The results of the wind-speed return period analysis are given in Table 4. In lengthening the open-water season to May to November and altering the distribution of peak storm wind speeds, by 2050, peak storm winds expected to occur in a given interval are likely to increase slightly. By 2100, with an open-water season from April to December and further altered distribution of peak storm winds, the peak speeds of storms with a given return period are again likely to increase slightly. The strongest storms (e.g., peak speeds over 95 km hr^{-1}, currently the 25-year wind event) are likely to increase in frequency by approximately 60% by 2100 such that the 25-year event could be expected to occur every 15 years, and the event expected every 100 years is likely to occur every 60 years.

Overall, the scenario suggests possible changing seasonality in forcing from a current maximum in August to September to a maximum in September to October by 2050 and October to November by 2100 when maximum storm surge frequencies, north-westerly wind storm frequencies, open-water extent and ice-bonded sediment thaw coincide. Frequency and severity of flooding of low-lying areas due to storm surges is very likely to increase. Given greater open-water extent, increased thaw of cliffs, increased storm surge elevations, and increased peak storm wind speeds, accelerated coastal change is likely in the Beaufort Sea. Change is expected to be expressed as increased rates of coastal cliff retreat and reorganization of spits; the latter may grow in length and height, become submerged or migrate landward depending upon local geology and sediment supply.

4 Conclusions

Measured and modelled time series of wind speeds and directions, water levels, sea-ice extent and temperatures were investigated to identify variability in past forcing of change of the Beaufort Sea shorelines and develop a scenario of future forcing.

Analysis of the Tuktoyaktuk tide gauge reveals a statistically significant RSL rise of 3.5 ± 1.1 mm y^{-1} since 1962, a

rate higher than determined by longer term geological studies. Both isostatic subsidence and eustatic rise probably contribute to this rise. Wind records indicate stormy periods during the early 1960s and late 1980s to early 1990s. Water-level records indicate periods of elevated water levels during the periods 1968 to 1975, 1980 to 1985 and after 1990. Sea-ice and temperature records both show a periodicity of approximately five-years that may be related. There are apparent but statistically insignificant trends towards more open water during the open-water season and warmer winters and longer summer warm periods.

A list of 88 north-westerly wind storms at Pelly Island with mean speeds >50 km h^{-1} during the June to October open-water season was developed. Annual storm frequencies were highest during the 1960 to 1966 period, a time of generally higher wind speeds. A list of 77 open-water season water-level events at Tuktoyaktuk >1.25 m (chart datum) was developed as well as a list of 51 open-water season surge events > 0.7 m and of six hours or longer duration. Peak storm-surge heights are correlated with peak storm wind speed, mean direction, minimum storm air pressure and percentage of open water with 69% of the variability explained by these four variables.

Return periods of wind and water-level events were calculated for the years of record and predicted for 2050 and 2100. Even though total storm frequency is likely to decrease slightly, the peak speeds of NWOW wind events expected to occur during a given time period are likely to increase slightly up to 2100 as the frequency of the most severe storms is likely to increase. The occurrence of severe flooding is very likely to increase considerably with the current 25-year water level occurring annually by 2100.

A future forcing scenario includes: very likely RSL rise of possibly 0.31 m by 2050 and 0.76 m by 2100; very likely decreased sea ice with an open-water season possibly being May to November by 2050 and April to December by 2100; unlikely change in storm tracks affecting the Beaufort; likely increased frequency of severe storms possibly occurring later in the year; likely overall increased wave energy with likely decreased wave energy during the summer months but increased wave energy during the winter months; and very likely increased air temperatures with greater warming during the winter months.

The results suggest possible changing seasonality in forcing from a current maximum during August to September to a maximum during September to October by 2050 and October to November by 2100 when maximum storm surge frequencies, north-westerly wind storm frequencies, open-water extent and ice-bonded sediment thaw coincide. With increased severity and frequency of forcing, accelerated rates of coastal change and increased occurrence and severity of flooding are likely along the shorelines of the Beaufort Sea.

Acknowledgements

Data were supplied by Environment Canada (the Meteorological Service of Canada, the Canadian Ice Service and the Canadian Centre for Climate Modelling and Analysis) and Fisheries and Oceans Canada (Pacific Tidal Section and Marine Environmental Data Service). Adam Macdonald assisted with the GIS analysis of ice data. James Young and Dave Hudak assisted by providing data and works in progress. Comments by Humfrey Melling, Dustin Whalen and two anonymous reviewers are gratefully acknowledged. This is Earth Sciences Sector Contribution No. 20060541.

Appendix

TABLE 1A. Wind events identified at Pelly Island with water level at Tuktoyaktuk, hindcast wave height off Pelly Island (Eid and Cardone, 1992), and open water in the Beaufort Sea. Dates are given as dd/mm/yyyy. Estimated values are identified with question marks.

Number	Date	Duration (hrs)	Mean Wind Speed (km h^{-1})	Peak Wind Speed (km h^{-1})	Mean Wind Direction	Peak Wind Direction	Max. Water Level (m above CD)	Peak Surge Height (m)	Sig. Wave Height (m)	% Open Water
0	09/09/1944	20?	–	95?	NW	–	2.4?	?	–	–
1	27/07/1959	7	52	52	290	290	–	–	–	–
2	01/08/1959	6	58	63	295	270	–	–	–	–
3	04/10/1959	13	60	73	310	320	–	–	–	–
4	25/07/1960	12	57	61	300	320	–	–	–	–
5	20/08/1960	18	59	61	290	290	–	–	–	–
6	14/09/1960	12	59	63	286	270	–	–	–	–
7	20/09/1960	24	54	59	314	320	–	–	–	–
8	29/09/1960	6	52	52	290	290	–	–	–	–
9	05/10/1960	12	59	63	290	290	–	–	–	–
10	28/07/1962	7	77	93	305	290	1.73	1.25	–	–
11	04/09/1962	18	67	83	292	290	2.15	1.55	–	–
12	05/07/1963	12	60	61	293	270	1.51	0.83	–	–
13	30/07/1963	25	69	76	308	320	1.89	1.50	–	–
14	27/08/1963	6	56	59	320	320	1.04	0.65	–	–
15	03/10/1963	7	56	83	306	290	2.23	1.85	–	–
16	16/10/1963	13	54	59	340	320	1.26	1.01	–	–
17	26/06/1964	24	65	67	320	320	1.03	0.48	–	–
18	19/07/1964	6	57	61	320	320	1.05	0.57	–	–
19	20/08/1964	18	59	61	320	320	1.22	0.59	–	–
20	04/09/1964	12	69	78	320	320	–	–	–	–

Table 1A. *(Continued)*

21	07/08/1965	13	67	78	327	320	1.7	1.31	–	–
22	21/09/1965	25	61	72	304	290	–	–	–	–
23	28/09/1965	12	57	61	300	290	–	–	–	–
24	10/09/1966	7	52	52	335	20	1.43	0.89	–	–
25	24/06/1967	7	61	63	290	290	1.04	0.51	–	–
26	24/07/1967	7	56	59	320	320	1.46	0.92	–	–
27	28/06/1968	6	52	52	330	320	–	–	–	3
28	04/10/1968	6	63	65	290	290	1.41	0.89	–	64
29	17/08/1969	7	60	78	332	270	1.42	0.80	–	16
30	21/08/1969	13	62	65	360	360	1.61	1.01	–	16
31	06/09/1970	7	57	59	330	320	–	–	–	84
32	14/09/1970	6	85	92	290	290	2.4?	?	4.21	45
33	12/10/1970	13	62	73	311	320	–	–	–	3
34	29/07/1971	7	60	61	280	270	1.36	0.84	–	40
35	02/09/1972	12	64	67	317	310	–	–	–	69
36	30/10/1972	6	59	59	295	280	–	–	–	0
37	20/08/1974	13	62	67	337	330	1.15	0.82	–	14
38	11/08/1975	13	61	67	293	300	1.67	1.16	3.27	27
39	27/08/1975	7	64	73	295	300	1.74	1.37	3.08	28
40	25/09/1975	6	52	52	300	290	1.08	0.71	–	4
41	28/10/1975	7	53	59	296	290	0.73	0.35	–	2
42	30/10/1975	13	51	52	303	300	0.7	0.32	–	2
43	06/07/1976	6	52	52	295	280	1.02	0.51	–	28
44	28/08/1977	12	61	65	287	280	–	–	2.61	82
45	16/09/1980	6	59	63	315	310	1.28	0.91	–	36
46	03/08/1981	6	61	63	325	340	1.98	1.47	2.85	52
47	17/08/1981	18	59	63	290	290	1.56	1.09	3.00	58
48	30/08/1981	36	59	63	314	290	1.62	1.04	2.68	71
49	17/09/1981	7	57	58	300	300	1.22	0.68	–	79
50	05/10/1981	24	63	68	304	310	1.35	1.00	–	60
51	21/08/1982	7	63	63	300	300	1.45	1.06	3.51	56
52	21/10/1982	25	67	87	280	270	–	–	3.51	30
53	23/09/1983	7	54	56	325	320	1.33	0.85	–	26
54	19/07/1984	12	59	63	280	290	1.46	0.84	–	14
55	12/08/1984	30	61	68	288	270	1.49	0.95	–	25
56	26/08/1984	36	69	82	348	340	1.59	0.96	2.97	26
57	25/10/1984	24	60	73	298	300	1.22	0.77	–	3
58	20/07/1985	7	59	63	310	310	1.12	0.47	–	10
59	17/09/1985	43	64	73	271	270	1.73	1.42	4.27	40
60	22/08/1986	7	54	87	310	330	1.79	1.54	3.45	40
61	05/10/1986	13	68	85	293	300	–	–	–	55
62	23/08/1987	6	59	60	285	290	0.82	1.54	–	77
63	31/08/1987	12	55	73	292	260	1.44	0.80	3.76	79
64	05/09/1987	6	66	73	305	310	1.4	1.02	–	68
65	04/08/1988	6	64	73	295	300	1.8	1.20	3.35	43
66	17/10/1988	12	61	68	277	270	–	–	–	7
67	16/09/1989	6	66	68	300	300	–	–	–	66
68	18/10/1989	7	59	63	335	330	–	–	–	44
69	02/09/1990	12	59	73	307	330	–	–	–	61
70	03/09/1990	6	57	60	280	280	–	–	–	58
71	08/09/1990	12	54	63	284	280	–	–	–	58
72	04/08/1991	6	64	68	360	10	1.19	0.63	–	18
73	24/08/1991	6	56	58	300	300	1.68	1.10	–	18
74	23/10/1991	6	82	91	290	280	–	–	–	2
75	23/09/1992	6	60	60	285	280	1.25	0.81	–	52
76	17/09/1993	15	61	73	313	320	1.68	1.24	–	91
77	22/09/1993	27	73	96	284	290	2.2	1.68	–	91
78	02/10/1993	15	58	73	277	280	1.18	0.69	–	91
79	13/10/1993	17	61	73	280	280	1.66	1.10	–	16
80	18/08/1994	7	70	87	270	270	1.9	1.52	–	42
81	22/08/1994	13	61	69	289	290	1.68	1.19	–	42
82	04/06/1996	6	55	61	291	290	0.89	0.50	–	0
83	27/08/1996	12	57	65	287	290	1.38	0.97	–	32
84	16/08/1998	8	58	70	275	290	–	–	–	90
85	27/08/1999	9	53	59	282	280	–	–	–	–
86	24/09/1999	14	55	69	303	300	–	–	–	–
87	25/09/1999	22	64	76	298	310	–	–	–	–
88	28/09/1999	11	55	65	309	300	–	–	–	–
89	10/09/2000	15	58	91	NW	–	2.18?	1.74?	–	50?

References

BERRY, M.O.; P.M. DUTCHAK, M.E. LALONDE, J.A.W. MCCULLOCH and I. SAVDIE. 1975. Weather, waves and icing in the Beaufort Sea. Beaufort Sea Technical Report 21, Department of the Environment, Ottawa, 123 pp.

BRYAN, K. 1996. The steric component of sea level rise associated with enhanced greenhouse warming: a model study. *Clim. Dyn.* **12**: 545–555.

CAMPEAU, S.; A., HEQUETTE and R. PIENITZ. 2000. Late Holocene diatom biostratigraphy and sea-level changes in the southeastern Beaufort Sea. *Can. J. Earth Sci.* **37**: 63–80.

CHURCH, J.A.; J.M. GREGORY, P. HUYBRECHTS, M. KUHN, K. LAMBECK, M.T. NHUAN, D. QIN, P.L. WOODWORTH, O.A. ANISIMOVM, F.O. BRYAN, A. CAZENAVE, K.W. DIXON, B.B. FITZHARRIS, G.M. FLATO, A. GANOPOLSKI, V. GORNITZ, J.A. LOWE, A. NODA, J.M. OBERHUBER, S.P. O'FARRELL, A. OHMURA, M. OPPENHEIMER, W.R. PELTIER, S.C.B. RAPER, C. RITZ, G.L. RUSSELL, E. SCHLOSSER, C.K. SHUM, T.F. STOCKER, R.J. STOUFFER, R.S.W. VAN DE WAL, R. VOSS, E.C. WIEBE, M. WILD, D.J. WINGHAM and H.J. ZWALLY. *Climate change 2001: the scientific basis. Contribution of Working Group I to the Third Assessment Report of the Intergovernmental Panel on Climate Change*. Cambridge University Press, Cambridge UK, pp. 639–693.

COUTURE, R.; S. ROBINSON, M. BURGESS and S. SOLOMON. 2002. Climate change, permafrost, and community infrastructure: a compilation of background material from a pilot study of Tuktoyaktuk, Northwest Territories. Geological Survey of Canada Open File D3867, 89 pp.

DALLIMORE, S.R.; S.A. WOLFE and S.M. SOLOMON. 1996. Influence of ground ice and permafrost on coastal evolution, Richards Island, Beaufort Sea coast, N.W.T. *Can. J. Earth Sci.* **33**: 664–675.

DPW. 1971. Beaufort Sea storm, September 13–16, 1970: Investigation of effects in the Mackenzie Delta Region. Engineering Programs Branch Report.

EID, B.M. and V.J. CARDONE. 1992. Beaufort Sea extreme waves study. Environmental Studies Research Funds Report 114. Calgary, 143 pp. and 5 Appendices.

FLATO, G.M.; G.J. BOER, W.G. LEE, N.A. MCFARLANE, D. RAMSDEN, M.C. READER and A.J. WEAVER. 2000. The Canadian Centre for Climate Modelling and Analysis global coupled model and its climate. *Clim. Dyn.* **16**: 451–467.

FLATO, G.M. and G.J. BOER. 2001. Warming asymmetry in climate change simulations. Geophys. Res. Lett. **28**: 195–198.

FORBES, D.L. and J.P.M. SYVITSKI. 1994. Paraglacial coasts. In: *Coastal Evolution: Late Quaternary Shoreline Morphodynamics*. R.J.W. Carter and C.D. Woodroffe (Eds), Cambridge University Press, Cambridge UK, pp. 373–424.

FORBES, D.L. and R.B. TAYLOR. 1994. Ice in the shore zone and the geomorphology of cold coasts. *Prog. Phys. Geogr*. **18**: 59–89.

FORBES, D.L.; J.D. ORFORD, R.W.G. CARTER, J. SHAW and S.C. JENNINGS. 1995. Morphodynamic evolution, self-organisation, and instability of coarse-clastic barriers on paraglacial coasts. *Mar. Geol.* **126**: 63–85.

GORDON, C.; C. COOPER, C.A. SENIOR, H.T. BANKS, J.M. GREGORY, T.C. JOHNS, J.F.B. MITCHELL and R.A. WOOD. 2000. Simulation of SST, sea ice extents and ocean heat transports in a version of the Hadley Centre coupled model without flux adjustments. *Clim. Dyn.* **16**: 147–168.

HARPER, J.R.; R.F. HENRY and G.G. STEWART. 1988. Maximum storm surge elevations in the Tuktoyaktuk region of the Canadian Beaufort Sea. *Arctic*, **41**: 48–52.

HECKERT, N.A. and E. SIMIU. 1996. Extreme wind distribution tails: A peaks over threshold approach. *J. Structural Engin*. **122**: 539–547.

HÉQUETTE, A.; M.H. RUZ and P.R. HILL. 1995. The effects of Holocene sea-level rise on the evolution of the southeast coast of the Canadian Beaufort Sea. *J. Coastal Res.* **11**: 494–507.

HÉQUETTE, A.; M. DESROSIERS, P.R. HILL and D.L. FORBES. 2001. The influence of coastal morphology on shoreface sediment transport under storm-combined flows, Canadian Beaufort Sea. *J. Coastal Res.* **17**: 507–516.

HILL, P.R.; A. HÉQUETTE and M.-H. RUZ. 1993. Holocene sea-level history of the Canadian Beaufort shelf. *Can. J. Earth Sci*. **30**: 103–108.

HILL, P.R.; P.W. BARNES, A. HÉQUETTE and M.-H. RUZ. 1994. Arctic Coastal Plain Shorelines. In: *Coastal Evolution: Late Quaternary Shoreline Morphodynamics*, R.W. Carter and C.D. Woodroffe (Eds), Cambridge University Press, Cambridge UK, pp. 341–372.

HILL, P.R. and S.M. SOLOMON. 1999. Geomorphologic and sedimentary evolution of a transgressive thermokarst coast, Mackenzie Delta region, Canadian Beaufort Sea. *J. Coastal Res.* **15**: 1011–1029.

HUDAK, D.R. and J.M.C. YOUNG. 2002. Storm climatology of the southern Beaufort Sea. ATMOSPHERE-OCEAN, **40**: 145–158.

HUNTINGTON, H.; G. WELLER, E. BUSH, T.V. CALLAGHAN, V.M. KATTSOV and M. NUTALL. 2005. An introduction to the Arctic Climate Impact Assessment. In: *Arctic Climate Impact Assessment*, C. Symon, L. Arris and B. Heal (Eds), Cambridge University Press, Cambridge, UK, pp. 1–19.

IPCC WG1. 2001. *Climate change 2001: the scientific basis. Contribution of Working Group I to the Third Assessment Report of the Intergovernmental Panel on Climate Change*. J.T. Houghton, Y. Ding, D.J. Griggs, M. Noguer, P. van der Linden, X. Dai, K. Maskell and C.I. Johnson (Eds), Cambridge University Press, Cambridge, UK, 882 pp.

JOHANNESSEN, O.M.; L. BENGTSSON, M.W. MILES, S.I. KUZMINA, V.A. SEMENOV, G.V. ALEEKSEEV, A.P. NAGURNYI, V.F. ZAKHAROV, L. BOBYLEV, L.H. PETTERSSON, K. HASSELMANN and H.P. CATTLE. 2002. Arctic climate change – observed and modelled temperature and sea ice variability. Nansen Environmental and Remote Sensing Centre Technical Report 218, 22 pp.

KATTSOV, V.M.; E. KÄLLÉN, H. CATTLE, J. CHRISTENSEN, H. DRANGE, I. HANSSEN-BAUER, T. JÓHANNESEN, I. KAROL, J. RÄISÄNEN. G. SVENSON, S. VAVULIN, D. CHEN, I. POLYAKOV and A. RINKE. 2005. Future climate change: modeling and scenarios for the Arctic. In: *Arctic Climate Impact Assessment*, C. Symon, L. Arris and B. Heal (Eds), Cambridge University Press, Cambridge, UK, pp. 100–144.

KOWALIK, Z. 1984. Storm surges in the Beaufort and Chukchi Seas. *J. Geophys. Res.* **89**: 10570–10578.

LAMBERT, S.J. 1995. The effect of enhanced greenhouse warming on winter cyclone frequencies and strengths. *J. Clim*. **8**: 1447–1452.

LAMBERT, S.J. 2004. Changes in winter cyclone frequencies and strengths in transient enhanced greenhouse warming simulations using two coupled climate models. ATMOSPHERE-OCEAN, **42**: 173–181.

LEWIS, P.J. 1987. Severe storms over the Canadian High Arctic: A catalogue summary for the period 1957 to 1983. Environment Canada, Ottawa, 285 pp.

LYNCH, A.H.; J.A. CURRY, R.D. BRUNNER and J.A. MASLANIK. 2004. Toward an integrated assessment of the impacts of extreme wind events on Barrow, Alaska. *Bull. Am. Meteorol. Soc.* **85**: 202–221.

MANSON, G.K.; D.L. FORBES and G.S. PARKES. 2002. Wave climatology. In: *Coastal Impacts of Climate Change and Sea-Level Rise on Prince Edward Island*. D.L. Forbes and R.W. Shaw (Eds), Geological Survey of Canada, Open File 4261, 31 pp. (on CDROM).

MANSON, G.K.; S.M. SOLOMON, D.L. FORBES, D.E. ATKINSON and M. CRAYMER. 2005. Spatial variability of factors influencing coastal change in the western Canadian Arctic. *Geomar. Lett.* **25**: 138–145.

MCCABE, G.J; M.P. CLARK and M.C. SERREZE. 2001. Trends in northern hemisphere surface cyclone frequency and intensity. *J. Clim.* **14**: 2763–2768.

MCFARLANE, N.A.; G.J. BOER, J.-P. BLANCHET and M. LAZARE. 1992. The Canadian Climate Centre second-generation general circulation model and its equilibrium climate. *J. Clim.* **5**: 1013–1044.

MURTY, T.S. and R.J. POLAVARAPU. 1979. Influence of an ice layer on the propagation of long waves. *Mar. Geodesy*, **2**: 99–125.

PANDEY, M.D.; P.H.A.J.M. VAN GELDER and J.K. VRIJLING. 2001. The estimation of extreme quantiles of wind velocity using L-moments in the peaks-over-threshold approach. *Structural Safety*, **23**: 179–192.

PELTIER, W.R. 1994. Ice age paleotopography. *Science*, **265**: 195–201.

RÄISÄNEN. J. 2001. CO_2-induced climate change in CMIP2 experiments: Quantification of agreement and role of internal variability. *J. Clim.* **14**: 2088–2104.

READER, C.M. and G.J. BOER. 1998. The modification of greenhouse gas warming by the direct effect of sulphate aerosols. *Clim. Dyn.* **14**: 593–608.

REISS, R.-D. and M. THOMAS. 2001. *Statistical Analysis of Extreme Values*. Birkhauser, Boston USA. 316 pp.

ROECKNER, E.; L. BENGTSSON, J. FEICHTER, J. LELIEVELD and H. RODHE. 1999. Transient climate change simulations with a coupled atmosphere-ocean GCM including the tropospheric sulfur cycle. *J. Clim*. **12**: 3004–3032.

RUZ, M.-H.; A. HÉQUETTE and P.R. HILL. 1992. A model of coastal evolution in a transgressed thermokarst topography, Canadian Beaufort Sea. *Mar. Geol.* **106**: 251–278.

SHAW, J.; R.B. TAYLOR, S.M. SOLOMON, H.A. CHRISTIAN and D.L. FORBES. 1998. Potential impacts of global sea-level rise on Canadian coasts. *Can. Geographer*, **42**: 365–379.

SOLOMON, S.M.; P.J. MUDIE, R. CRANSTON, T. HAMILTON, S.A. THIBAUDEAU and E.S. COLLINS. 2000. Characterisation of marine and lacustrine sediments in a drowned thermokarst embayment, Richards Island, Beaufort Sea, Canada. *Int. J. Earth Sci.* **89**: 503–521.

WANG, X.L. and V.R. SWAIL. 2006. Climate change signal and uncertainty in projections of ocean wave heights. *Clim. Dyn.* **26**: 109–126.